

Multiresonant ZVS Boost Converter

Elżbieta SZYCHTA

Technical University of Radom, Poland

Summary: The article presents properties of multiresonant voltage-increasing converter to be applied in DC voltage supply systems. The configuration of the system elements enables application of the technique of zero voltage switching (ZVS) of semi-conductor elements, which yields high operating frequencies of the system while maintaining high energy efficiency and reliability of operation. Results of simulation tests of the converter, based on Simplorer, are discussed. Regulation characteristics are presented and the converter's efficiency is determined.

Keywords: multiresonant converter, zero voltage switching (ZVS), resonant circuits

1. INTRODUCTION

In energy-saving resonant power processing systems, switching of semi-conductor power elements occurs at high frequency and zero voltage (ZVS) or zero current (ZCS) [1]. Energy efficiency of such converters depends, to a large extent, on the transistor and diode switching processes. Power losses at turn on and off result from the current in the switched system multiplied by the voltage in switched semi-conductor elements.

What is characteristic of quasi-resonant ZCS converters is their ability to switch off the transistor at zero value of the current [8]. The transistor is switched on at the supply voltage of the converter. Losses due to impact of the transistor's parasitic capacitance called occur then (switching Miller effect) [4]. Rectifying diode is switched off at zero current. Maximum operating frequency of quasi-resonant ZCS converters is limited above all by the losses connected to transistor turn-on, and is up to 2 MHz [15].

What is characteristic of quasi-resonant ZVS converters is their ability to switch off the transistor at zero value of the voltage [14]. Voltage stresses occur when the rectifying diode is switched, causing parasitic oscillations between the diode's parasitic capacitance and resonant inductance. These oscillations cause losses at high switching frequencies and adversely affect the system's stability. The conditions of semi-conductor element switching enable operation of quasi-resonant ZVS converter at operating frequencies up to 10 MHz [15].

ZCS and ZVS quasi-resonant converters allow for switching at zero value of current or voltage of the transistor or diode, but not of both the elements at the same time. These systems experience undesirable oscillations of resonant current caused by parasitic capacitances of semi-conductor elements and inductances of connections. This limits the potential for application of quasi-resonant converters to power processing at high switching frequency [14].

Further research into analysis of properties of resonant system structures where all semi-conductor elements would be switched at soft commutation of voltages or currents led to development of multiresonant converters [1,2,5,7,14]. Design of these converters features controlled switches, including MOSFET transistor, rectifying diode and resonant circuit overloading at two different frequencies. Load

resistance of the converter is an element of the resonant circuit. Parasitic capacitances of the transistor and diode, leakage inductance of transformer, and connection inductances are all parts of the resonant circuit. Semi-conductor elements are switched at zero voltage (ZVS) or zero current (ZCS).

Designs of multiresonant converters operating at zero voltage of the transistor and diode (ZVS) should be characterized by the following properties (Fig. 1):

1. Resonant capacitance C_S is located parallel with the transistor T. When the transistor conducts, capacitance C_S is not a part of the system's operation. When the transistor does not conduct, capacitance C_S and parasitic capacitance of the transistor C_{0S} , in parallel, conduct resonant current of the converter.
2. Resonant capacitance C_D is located parallel with the rectifying diode D. When the diode conducts, capacitance C_D is not a part of the system's operation. When the diode does not conduct, capacitance C_D and parasitic capacitance of the diode C_{0D} , in parallel connection, conduct resonant current of the converter.
3. Resonant inductance L is part of the circuit including the transistor and diode D. The circuit can also comprise a voltage source and filter capacitances and inductances.

Application of ZVS method in multiresonant converters produces high operating frequencies of such systems, enables elimination of parasitic oscillations of the current in resonant circuit, restricts dynamics of voltage and current stresses, and minimizes power losses [1]. Multiresonant ZVS converters can be applied in systems supplying DC voltage electricity, where high energy efficiency is a requirement.

Basic designs of multiresonant converters are presented in references [15, 17]. Results of tests of forward converter are discussed in [17]. Buck converter is analysed in [11,14].

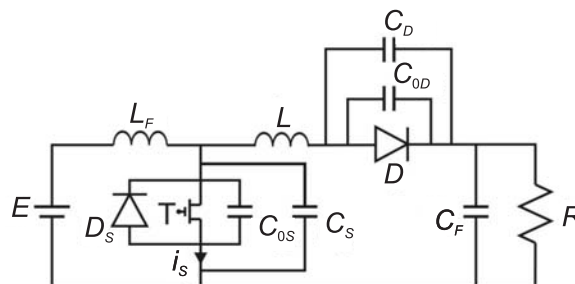


Fig.1. Multiresonant ZVS boost converter

Interesting properties of the other converter designs require detailed analysis. This article discusses multiresonant ZVS boost converter.

2. TOPOLOGY OF MULTIRESONANT ZVS BOOST CONVERTER

Multiresonant ZVS boost converter is shown in Figure 1.

A high inductance L_F choke, in series with a voltage source E , supplies the converter with current. Transistor MOSFET T , with resistance R_T when conducting and output

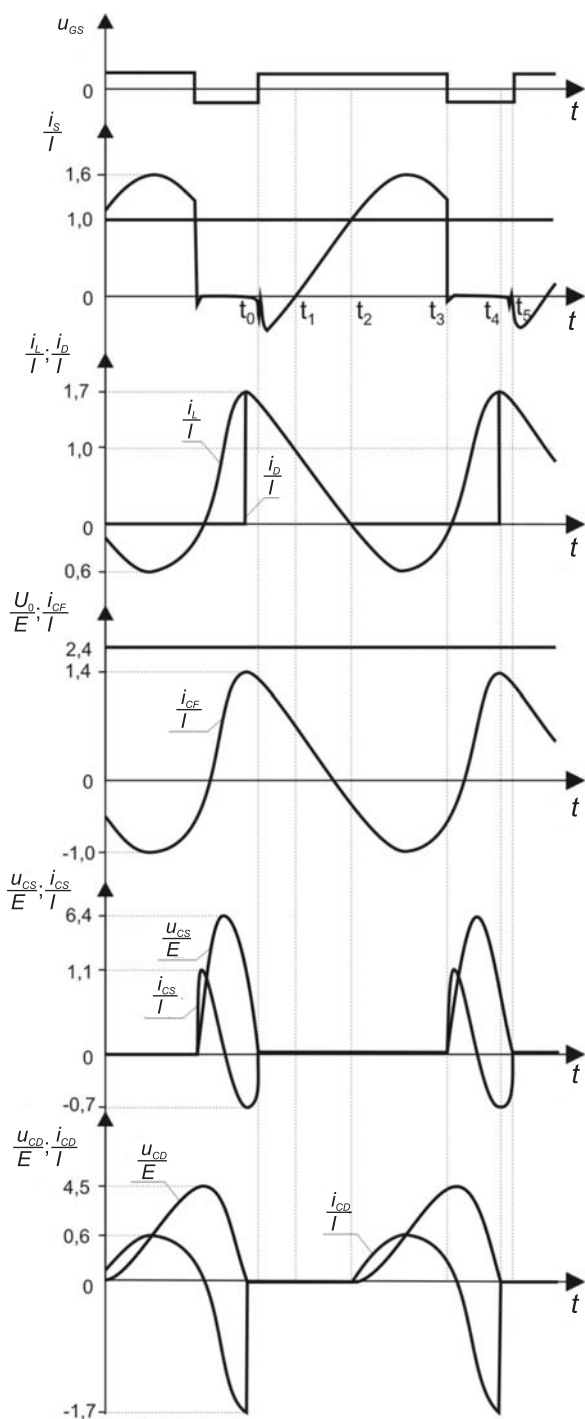


Fig. 2. Current and voltage waveforms in the converter, relative units

capacitance C_{0S} , is switched at frequency f . Diode D_S is an integral part of the transistor and enables two-way conduction of current i_S in a transistor leg. The rectifying diode D contains parasitic output capacitance C_{0D} . The converter's resonant circuit includes the following elements: choke with inductance L , capacitance C_S in parallel with the transistor, and capacitance C_D , in parallel with the diode D . Elements of the resonant circuit cooperate with the system's parasitic reactances, that is, inductance L 'absorbs' leak reactance of the transformer, and capacitances C_S and C_D in parallel connections 'absorb' parasitic capacitances C_{0S} , C_{0D} . The value of capacitance C_S should be much greater than that of the parasitic capacitance C_{0S} in order for the capacitance C_S to take over most part of the resonant current. Choice of a transistor of the lowest possible output capacitance C_{0S} contributes to greater efficiency of the system [1]. Configuration of the system elements allows for application of zero voltage switching of both the transistor and the diode. Capacitance C_F is a low-pass filter that limits pulsation of output voltage.

When the transistor is conducting, the capacitance C_S is not involved in conduction of resonant current. At high quality factor of the system, frequency of oscillations f_D of the resonant circuit R, L, C_D, C_{0D} is:

$$f_D = \frac{1}{2\pi\sqrt{L(C_D + C_{0D})}} \quad (1)$$

When the diode D is conducting, the capacitance C_D is not involved in conduction of resonant current. At high quality factor of the system, frequency of oscillations f_S of the resonant circuit R, L, C_S, C_{0S} is:

$$f_S = \frac{1}{2\pi\sqrt{L(C_S + C_{0S})}} \quad (2)$$

3. DESCRIPTION OF THE SYSTEM'S OPERATION

In a boost system (Fig. 1), an operating cycle is divided into five time intervals. Current and voltage waveforms, in relative units, during the cycle are illustrated in Figure 2. Resonant circuits for particular intervals are shown in Figure 3.

In the first time interval ($t_0 \leq t \leq t_1$) (Fig. 2), at the moment $t = t_0$, the transistor is switched on to operate. The equation: $I = i_L + i_S$ obtains for node 1 (Fig. 3a). The value of resonant current i_L is greater than that of the supply current I . Current $I = \text{const.}$, thus the difference of currents $i_L - I$ is conducted by the diode D_S of the transistor. Energy occurring in the choke L at $t = t_0$ is passed on to the capacitance C_F in the circuit: L, D, C_F, D_S . When the current i_L reaches the value I , diode D_S stops conducting and the system moves on to the second operating range, and voltages of the drain - source transistor u_{CS} and of the diode u_{CD} equal zero.

In the second time interval ($t_1 \leq t \leq t_2$) (Fig. 2), at $t = t_1$, the current $i_L = I$, the current $i_S = 0$ and the transistor begins to conduct (Fig. 3b). Energy stored in the choke L at $t = t_1$ continues to be transferred to the capacitance C_F in the circuit: L, D, C_F, I . At $t = t_2$, the current $i_L = 0$, the current i_S

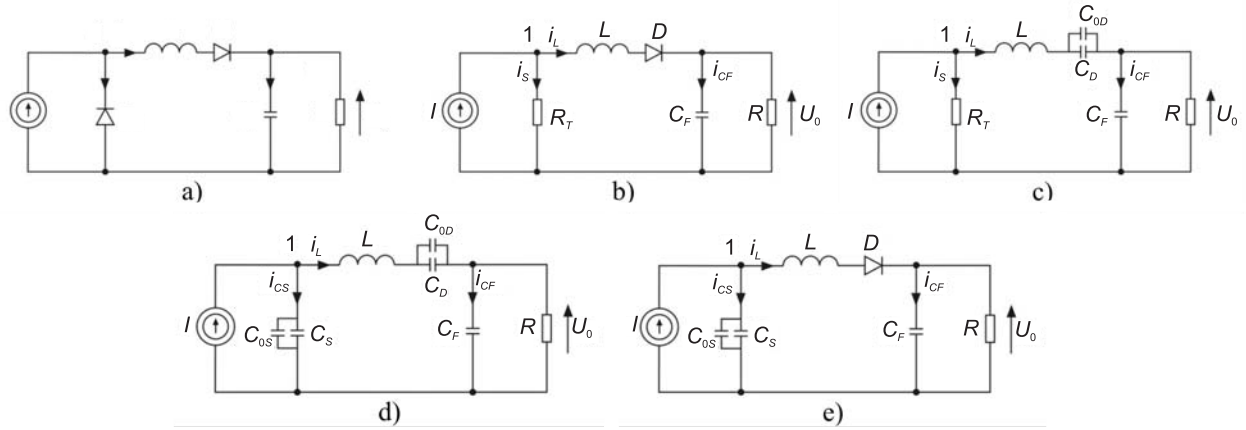


Fig. 3. Resonant circuit of the system shown in Fig. 1 a) first interval, b) second interval, c) third interval, d) fourth interval e) fifth interval

$= I$, voltages of the drain – source transistor u_{CS} and of the diode u_{CD} equal zero.

In the third time interval ($t_2 \leq t \leq t_3$) (Fig. 2) the transistor continues to conduct (Fig. 3c). The output voltage U_0 is greater than that of the transistor u_{CS} and a resonant circuit arises: $R_T, C_F, (C_D+C_{0D}), L$. Current of the transistor $i_S = I - i_L$. At $t = t_3$ the transistor is switched off (at zero voltage u_{CS}).

In the fourth time interval ($t_3 \leq t \leq t_4$) (Fig. 2), the transistor and the diode D are not conducting (Fig. 3d). The capacitance C_S and parasitic capacitance C_{0S} and the capacitance C_D and parasitic capacitance C_{0D} overload with the resonant current i_L . The equation: $I = i_L + i_{CS}$ obtains for node 1 (Fig. 3d). the process of oscillatory overload of the current i_L continues until $t = t_4$, when $u_{CD} = 0$.

In the fifth time interval ($t_4 \leq t \leq t_5$) (Fig. 2), at $t = t_4$ the diode D begins to conduct (Fig. 3e). The capacitance C_S and parasitic capacitance C_{0S} are conducting the current i_{CS} till $t = t_5$, when $u_{CS} = 0$. The transistor is ready to be turned on in the following cycle of the converter's operation.

Multiresonant ZVS converter is characterised by the following properties:

$$\begin{aligned}
 f_N &= \frac{f}{f_S} \\
 C_N &= \frac{C_D + C_{0D}}{C_S + C_{0S}} \\
 M &= \frac{U_0}{E} \\
 R_N &= \frac{R}{Z_S} \\
 Z_S &= \sqrt{\frac{L}{(C_S + C_{0S})}}
 \end{aligned} \tag{3}$$

where:

f — operating frequency of the converter,

f_N — operating frequency, relative units,

C_N — capacitance factor,

M — voltage conversion factor (output voltage, relative units),

U_0 — output voltage of the converter,

R_N — load resistance, relative units,

Z_S — characteristic impedance [1].

The power P_{we} received by the converter is:

$$P_{we} = I * E \tag{4}$$

where:

I — mean value of converter supply current.

Power P_{wy} released in load resistance R of the converter is:

$$P_{wy} = \frac{U_0^2}{R} \tag{5}$$

Efficiency of the converter η is:

$$\eta = \frac{P_{wy}}{P_{we}} \tag{6}$$

The magnitudes represented in the system of equations (3) are necessary to determine regulating characteristics of the converter. In view of complex mathematical apparatus, these characteristics can be determined using simulation tests.

4. SIMULATION TESTS

Multiresonant ZVS converter (Fig. 4) was subjected to Simplorer-based simulation tests. The simulation system comprised a MOSFET transistor IRFP460 (output capacitance $C_{0S} = 870\text{pF}$), and an ultrafast diode HFA25TB60 (output capacitance $C_{0D} = 100\text{pF}$) of International Rectifier. The resonant circuit contains the following element values: $L = 7\mu\text{H}$, $C_S = 7\text{nF}$, $C_D = 23\text{nF}$, $L_F = 600\mu\text{H}$, $C_F = 10\mu\text{F}$, $R = \text{var}$. On the basis of equations (1) and (2), resonant frequencies are: $f_S = 678\text{kHz}$, $f_D = 396\text{kHz}$. Supply voltage $E = 50\text{V}$.

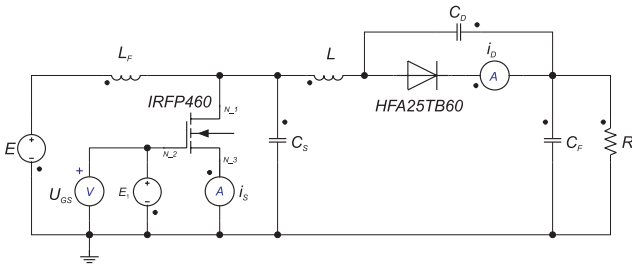


Fig. 4. Simulation model of multiresonant ZVS (boost) converter

The range of operating frequencies f which ensures ZVS switching in the converter at $C_N = 2,9$, $R = 30\Omega$ is $338\text{kHz} \leq f \leq 535\text{kHz}$. Frequency f can be increased through reduction of the transistor's conducting time. Minimum frequency $f_{min} = 338\text{kHz}$ obtains at the transistor's conducting time $t_{max} = 2,2\mu\text{s}$ and depends on the value of capacitance factor C_N . Figure 5 shows current and voltage waveforms during converter's steady operation at frequency $f = 338\text{kHz}$. Current and voltage waveforms in the steady condition are stable in nature. The waveform of transistor current i_s displays slight oscillations related to presence of the output capacitance C_{OS} . Transistor switching occurs at zero value of voltage u_{CS} .

Fall of frequency f below $f_{min} = 338\text{kHz}$ at $C_N = 2,9$ causes the system to become unstable, i.e. the converter is no longer capable of ZVS switching. The case of the loss of system stability is illustrated in Figure 6. Maximum frequency $f_{max} = 535\text{kHz}$ occurs at transistor's conducting time $t_{min} = 1\mu\text{s}$ and depends on the value of the transistor's parasitic capacitance. At frequencies f over the value $f_{max} = 535\text{kHz}$, major impact of parasitic capacitances on the system's operation becomes noticeable (Fig. 8). Within the range of operating frequencies $338\text{kHz} \leq f \leq 535\text{kHz}$, output voltage U_0 changes within the range $130,6\text{V} \geq U_0 \geq 59,7\text{V}$, supply current $13,1\text{A} \geq I \geq 2,6\text{A}$. Values of maximum voltages in the transistor and the diode occur within the ranges: $326\text{V} \geq U_{CSmax} \geq 185\text{V}$ and $246\text{V} \geq U_{CDmax} \geq 42\text{V}$.

Figure 8 shows selected regulating characteristics obtained as a result of simulation tests: $M = f(f_N)$, $I_{Smax}/I_0 = f(f_N)$, $U_{CSmax}/E = f(f_N)$, $U_{CDmax}/E = f(f_N)$. Each characteristic is presented for the range of operating frequency $f_{minN} \leq f_N \leq f_{maxN}$ which guarantees ZVS switching. The range of operating frequency f_N is variable and dependent upon load resistance R_N . Drop of frequency f_N below f_{minN} causes the system to lose its stability (Fig. 6). At values of frequency f_N over f_{maxN} parasitic capacitances have significant influence on the system's operation and increase of switching losses (Fig. 7).

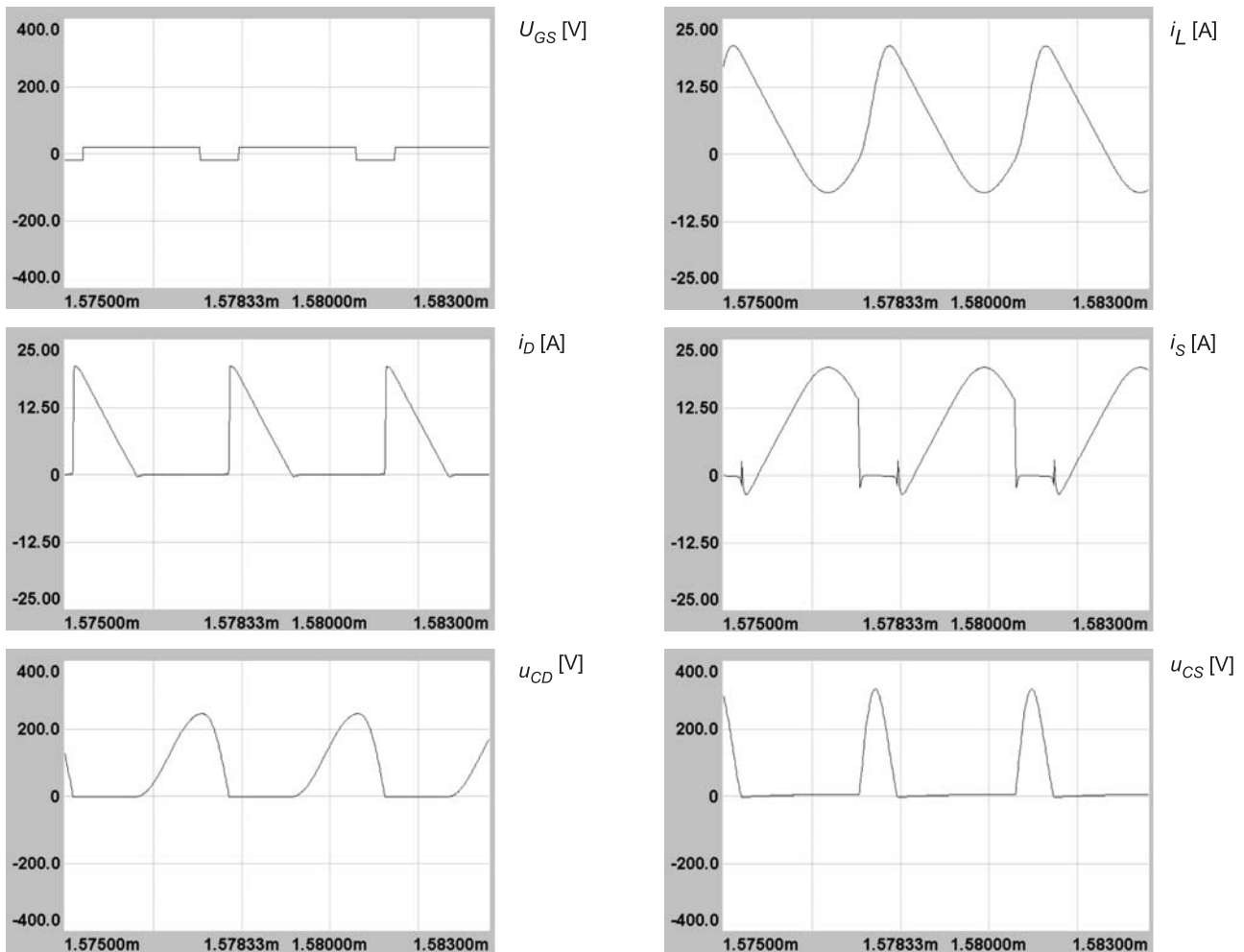


Fig.5. Current and voltage waveforms in the converter obtained during simulation, $C_N = 2,9$, $f = 338\text{kHz}$, $R = 30\Omega$

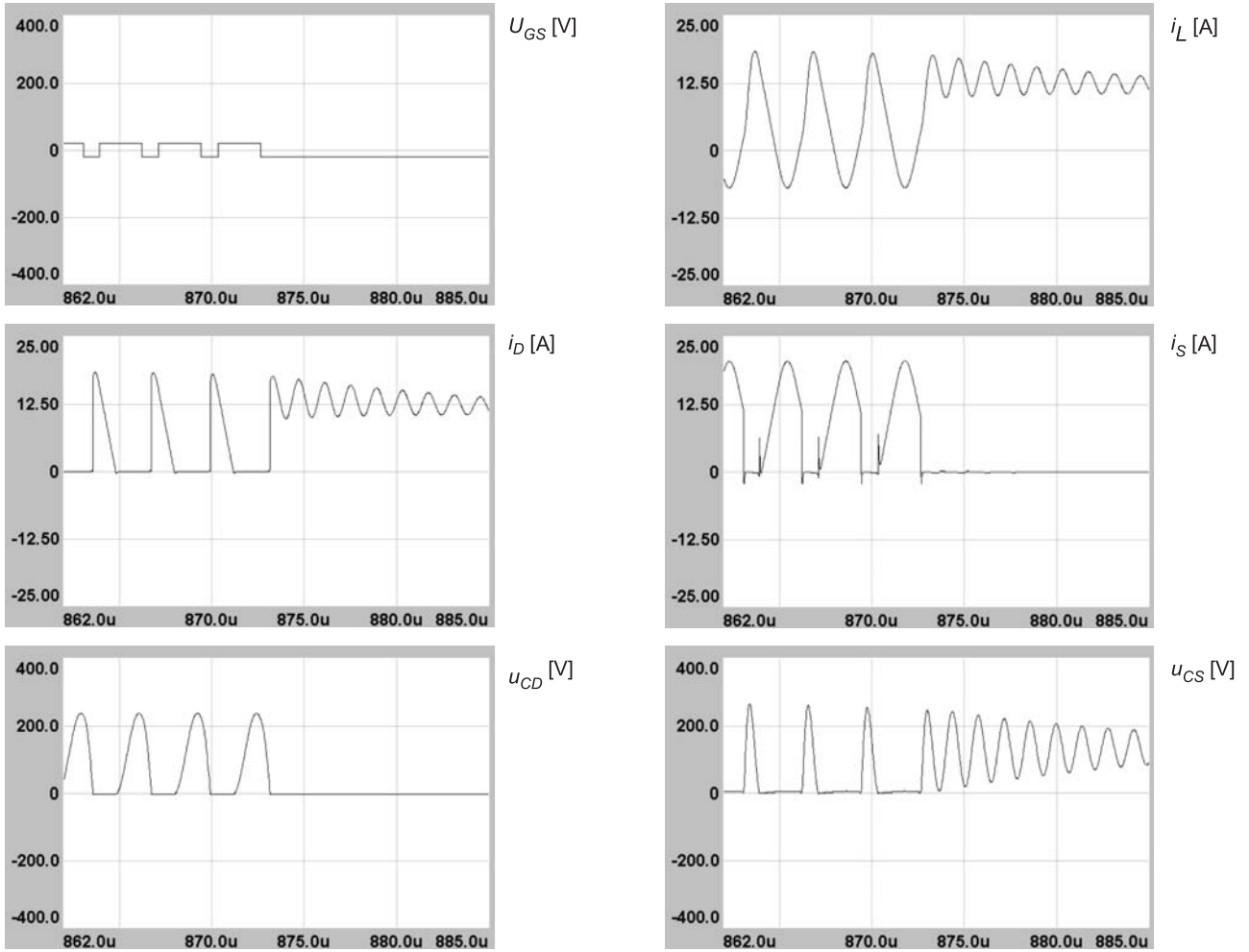


Fig. 6. Loss of converter's stability, $C_N = 2,9$, $f = 303\text{kHz}$, $R = 30\Omega$

Rise of relative frequency f_N causes reduction of the values of: factor M , maximum voltages in the transistor U_{CSmax}/E and the diode U_{CDmax}/E as well as maximum transistor's current I_{Smax}/I_0 (Fig. 8). Growth of resistance R_N leads to increase in values of: factor M , maximum voltages in the transistor U_{CSmax}/E and the diode U_{CDmax}/E as well as maximum transistor's current I_{Smax}/I_0 , with increased value of relative frequency f_N and reduced range f_N that ensures zero voltage switching.

Figure 8 indicates that at $C_N = 2,9$, $R_N = 1$, in the frequency range $0,50 \leq f_N \leq 0,79$ ($338\text{kHz} \leq f \leq 535\text{kHz}$), conversion factor of the converter M fits into the range: $2,6 \geq M \geq 1,2$, maximum voltage values in the transistor U_{CSmax}/E are within the range: $6,5 \geq U_{CSmax}/E \geq 3,7$, maximum voltage values in the diode U_{CDmax}/E are within the range: $4,9 \geq U_{CDmax}/E \geq 1,8$, maximum current values of the transistor fit in the range: $4,6 \geq I_{Smax}/I_0 \geq 2,6$.

Simulation testing confirms impact of parasitic capacitances of the transistor and of the diode, and of the value of factor C_N on the converter's stability. Value of capacitance factor C_N increases through growth of capacitance C_D (bearing in mind the existence of parasitic capacitance C_{0D}). Simulation tests of the transistor's conducting time $t_{max} = 2,1\mu\text{s}$, $R = 30\Omega$, $C_D = \text{var}$ showed that the converter's operation is stable if $2,6 \leq C_N \leq 6,4$. When the value C_N increases, load voltage varies in the

range $128\text{V} \geq U_0 \geq 78\text{V}$, supply current I changes within the range $12,4\text{A} \geq I \geq 4,7\text{A}$. The system's efficiency fits into the range $0,88 \geq \eta \geq 0,86$.

The higher the factor C_N , the lower the maximum value of resonant current i_L in the inductance L , the higher the conductance losses, and thus the lower the system's efficiency η . Growth of factor C_N leads to reduction of maximum voltage value U_{CDmax} in the diode. Major impact of changes of factor C_N on variation of operating frequency f and maximum voltage values U_{CSmax} in the transistor is not observed.

Simulation testing of the impact of load fluctuations on the system's operation demonstrates, that reduction in value of resistance R causes reduced frequency f , lower value of current I and of voltage U_0 . The higher the value of resistance R , the higher the maximum voltage values in the transistor U_{CSmax} and the diode U_{CDmax} , and the higher the maximum current values of the transistor I_{Smax} . At $C_N = 2,9$, $t_{max} = 2,1\mu\text{s}$, when values of resistance vary in the range $10\Omega \leq R \leq 30\Omega$, frequency f changes in the range $343\text{kHz} \leq f \leq 358\text{kHz}$, voltage U_0 fluctuates in the range $55\text{V} \leq U_0 \leq 120\text{V}$, voltage I changes in the range $6,54\text{A} \leq I \leq 10,9\text{A}$, the system's efficiency is within the range $0,92 \geq \eta \geq 0,88$.

Figure 9 illustrates efficiency of the converter ζ in function of relative frequency f_N in the range of operating frequency which ensures ZVS switching. Figure 9 shows, that efficiency ζ of the system declines as relative resistance R_N grows at

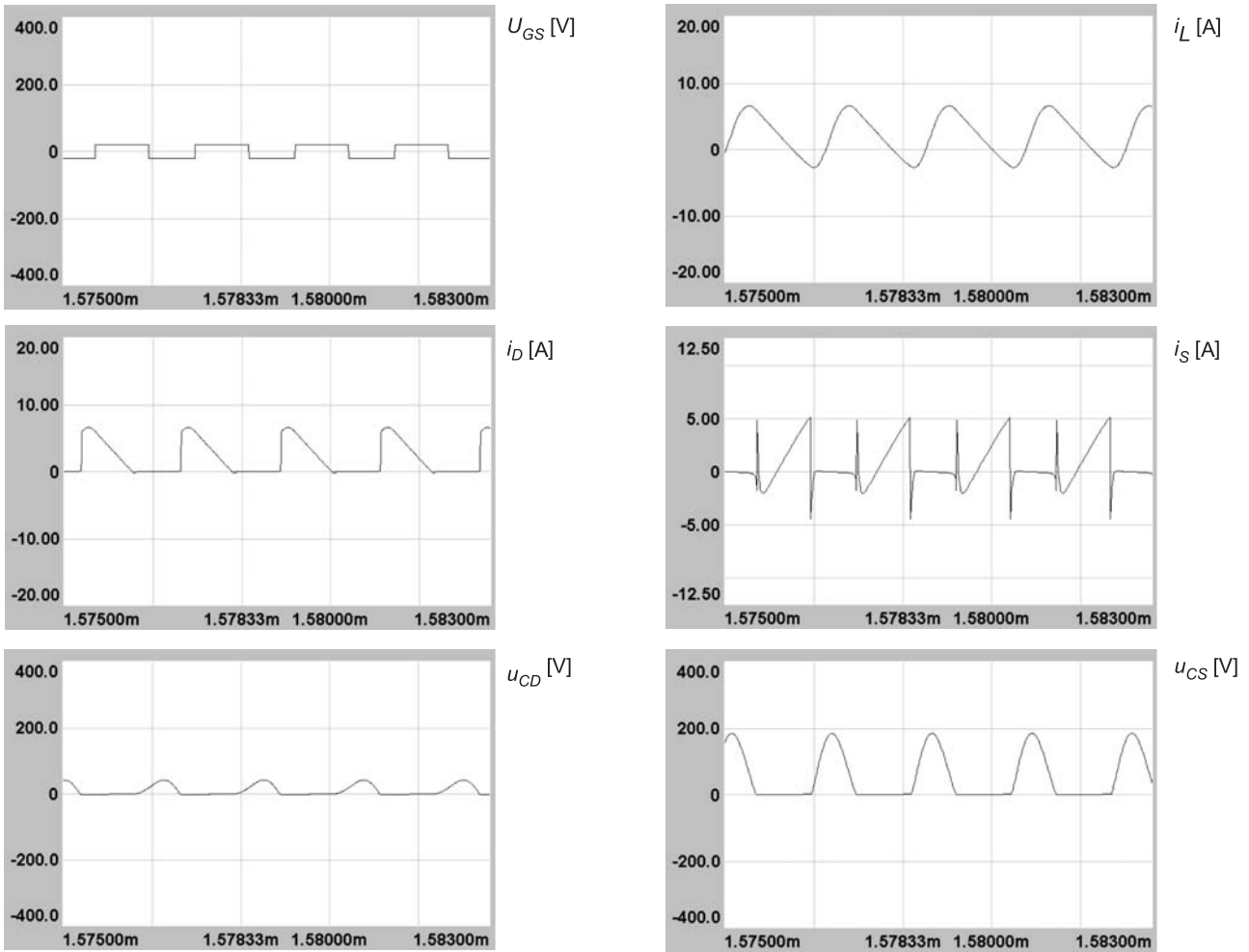


Fig.7. Current and voltage waveforms in the converter obtained during simulation, $C_N = 2,9$, $f = 535\text{Hz}$, $R = 30\Omega$

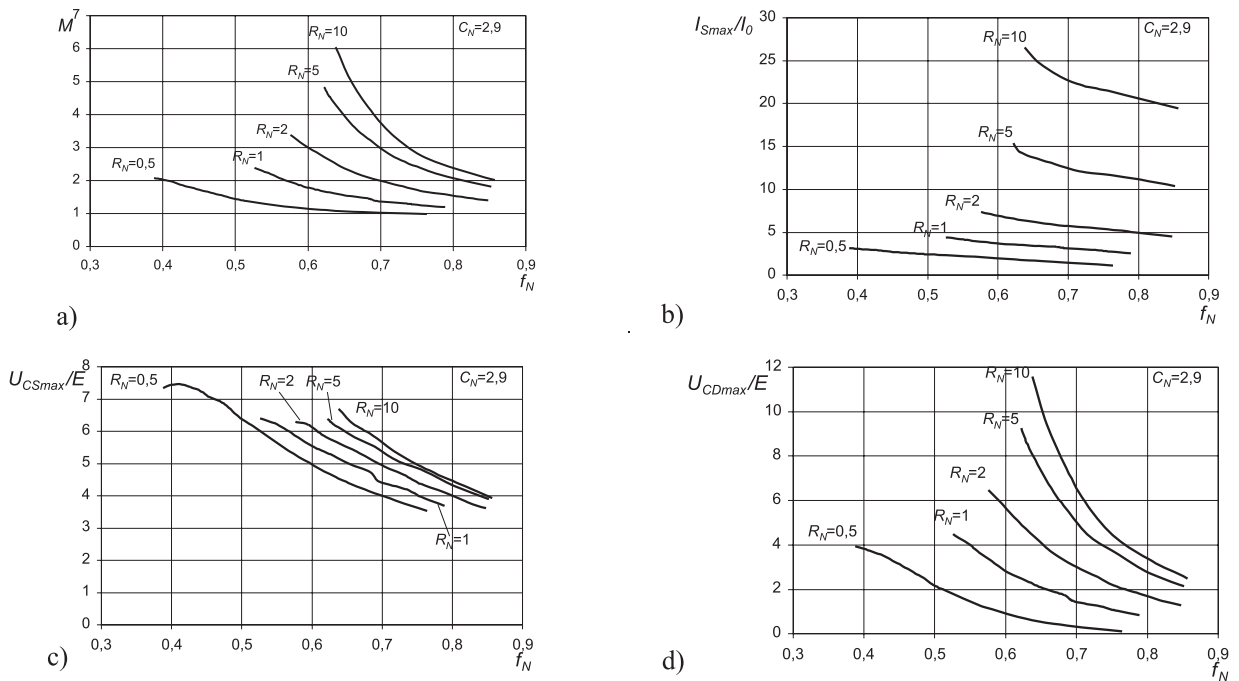


Fig. 8. Regulation characteristics for voltage boost converter, relative units, $C_N = 2,9$, a) conversion factor M , b) maximum transistor currents I_{Smax}/I_0 , c) maximum voltages in the transistor U_{CSmax}/E , d) maximum voltages in the diode U_{CDmax}/E

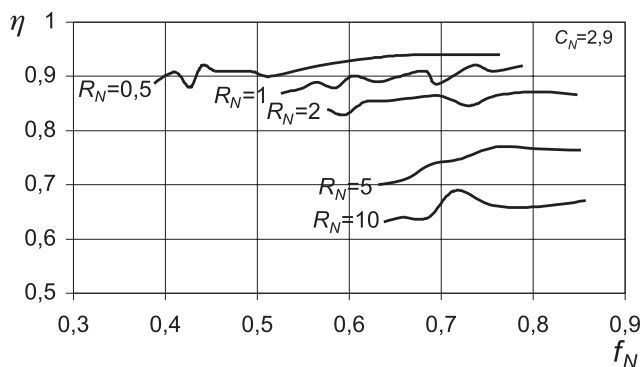


Fig. 9. Efficiency η of multiresonant ZVS boost converter, $C_N = 2,9$

$C_N = \text{const.}$ At $R_N = \text{const.}$, growth of frequency f_N causes the efficiency η to increase. It is especially felt at greater values of R_N .

5. CONCLUSION

Simulation testing of the analysed system yields the following conclusions:

1. Multiresonant ZVS boost converter provides good zero-voltage switching conditions for both the transistor and the diode. Parasitic capacitances of the transistor and the diode, parasitic inductances of connections, and leakage inductance of transformer are all part of the resonant circuit.
2. Switching of the transistor and the rectifying diode at zero voltage in the converter enables high operating frequency of the system while high energy efficiency is maintained.
3. The range of the converter's operating frequency in which ZVS switching is assured, determined on the basis of simulation testing, is variable and dependent on the load resistance.
4. Stability of the converter, defined as the ability to switch semi-conductor elements in cooperation with the resonant circuit, is maintained in the range of operating frequencies determined in regulation characteristics. Drop of the frequency below values within the system's operating range causes the system to lose its stability. A choice of resonant capacitances suited to conditions of the system's power supply and load, influences stability of the system.
5. Increase of operating frequencies above values within the system's operating range, shown in regulating characteristics, intensifies influence of parasitic capacitance on the system's efficiency.
6. Multiresonant ZVS boost converter generates DC voltage and can be applied in power supply systems where high energy efficiency is required.
7. Maximum voltage values in the transistor and the diode grow small, as the system's operating frequency rises or the value of load resistance falls.
8. Tests should continue using a real model in order to verify and confirm simulation results at the conditions of the converter's power supply and load.

REFERENCES

1. Citko T., Tunia H., Winiarski B.: Układy rezonansowe w energoelektronice (*Resonant Systems in Power Electronics*). Politechnika Białostocka Publications, Białystok 2001.
2. El-Bachtiri R., Matagne E., Labrigue F.: *Commutation processes in a multiresonant ZVS bridge inverter regulated by phase shifting the control of the two legs*. Electrotechnical Conference, 1996. MELECON '96., 8th Mediterranean, Volume 3, Issue -, Date: 13-16 May 1996, p. 1275-1278 vol. 3.
3. Farrington R., Jovanovic M.M., Lee F.C.: *Comparison of single-ended-parallel MRC and forward MRC*. Applied Power Electronics Conference and Exposition, 1992. APEC '92. Conference Proceedings 1992., Seventh Annual.
4. Januszewski S., Świątek H., Zymmer K.: *Półprzewodnikowe przyrządy mocy (Semi-conductor Power Devices)*. Warsaw. 1999, WKŁ.
5. Jovanovic M.M., Tabisz W.A., Lee F.C.: *Zero-voltage-switching technique in high-frequency off-line converters*. Applied Power Electronics Conference and Exposition, 1988. APEC '88. Conference Proceedings 1988., Third Annual IEEE Volume -, Issue -, Date: 1-5 Feb 1988, p. 23-32.
6. Kim H.J., Leu C.S., Farrington R., Lee F.C.: *Clamp mode zero-voltage-switched multi-resonant converters*. Power Electronics Specialists Conference, 1992. PESC '92 Record., 23rd Annual IEEE Volume, Issue, Date: 29 Jun-3 Jul 1992, p. 78-84 vol.1.
7. Kirchenberger U., Schroder D.: *Comparison of multiresonant half-bridge DC-DC converters for high voltage and high output power*. Industry Applications Society Annual Meeting, 1992., Conference Record of the 1992 IEEE Volume -, Issue -, Date: 4-9 Oct 1992, p. 902-909 vol. 1.
8. Nuno F., Diaz J., Sebastian J., Lopera J.: *A unified analysis of multi-resonant converters*. Power Electronics Specialists Conference, 1992. PESC '92 Record., 23rd Annual IEEE Volume, Issue, Date: 29 Jun-3 Jul 1992, p. 822-829 vol. 2.
9. Schoneman G.K.: *A novel zero-voltage switched multiresonant converter*. Power Electronics Specialists Conference, 1991. PESC '91 Record., 22nd Annual IEEE Volume, Issue, Date: 24-27 Jun 1991, p. 195-201.
10. Szychta E.: Wpływ pojemności wyjściowych tranzystorów typu MOSFET na pracę jednofazowego szeregowego falownika napięcia (*Impact of Output Capacitances of MOSFET Transistors on Operation of One-phase, Series Voltage Inverter*). Przegląd Elektrotechniczny, No. 4, 2005.
11. Szychta E.: Własności multirezonansowego przekształtnika ZVS obniżającego napięcie (*Properties of Multiresonant ZVS Buck Converter*). SENE 2005.
12. Szychta E.: Własności multirezonansowych przekształtników DC (*Properties of Multiresonant DC Converters*). Przegląd Elektrotechniczny, in the press.
13. Szychta E.: *ZVS multiresonant converter to be applied in power supply systems of telematics equipment*. Katowice 2005.
14. Tabisz W.A., Lee F.C.: *DC analysis and design of zero-voltage-switched multi-resonant converters*. Power Electronics Specialists Conference, 1989. PESC '89 Record., 20th Annual IEEE Volume, Issue, Date: 26-29 Jun 1989, p. 243-251 vol.1.
15. Tabisz W.A., Lee F.C.Y.: *Zero-voltage-switching multiresonant technique-a novel approach to improve performance of high-frequency quasi-resonant converters*, Power Electronics, IEEE Transactions 4/4, Date: Oct 1989, p. 450-458.
16. Tang W., Leu C.S., Lee F.C.: *Charge control for zero-voltage-switching multiresonant converter*. Power Electronics, IEEE Transactions 11/2, Date: Mar 1996, p. 270-274.
17. Tang W., Tabisz W.A., Lotfi A., Lee F.C., Vorperian V.: *DC analysis and design of forward multiresonant converter*. Power Electronics Specialists Conference, 1990. PESC '90 Record., 21st Annual IEEE Volume, Issue, Date: 11-14 Jun 1990, p. 862-869.



Elżbieta Szychta

Graduated from the Electrical Faculty of Warsaw Polytechnic in 1981. Obtained a degree of doctor of engineering from the Electrical Faculty of Warsaw Polytechnic in 1988. Since 1981 she has worked for the Transport Faculty Kazimierz Pułaski at the Technical University of Radom. An assistant professor in the Department of Electrical Machinery and Equipment. Interested in industrial power electronics.

Address: Politechnika Radomska, Wydział Transportu, 26-600 Radom, ul. Malczewskiego 29; tel: (048) 361 77 00, e-mail: e.szychta@pr.radom.pl